Materials Research
Express

PAPER • **OPEN ACCESS**

Investigation & analysis of Electrical Discharge Machining on Titanium Diboride Ceramic material with various Electrode materials and dielectric fluids

To cite this article: Karthik S and Sivakumar Annamalai 2025 *Mater. Res. Express* **12** 016501

IOP Publishing Mater. Res. Express 12 (2025) 016501 https://doi.org/10.1088/2053-1591/ada10e

Materials Research Express

PAPER

OPEN ACCESS

RECEIVED
3 September 2024

REVISED
10 December 2024

ACCEPTED FOR PUBLICATION
18 December 2024

PUBLISHED
10 January 2025

Investigation & analysis of Electrical Discharge Machining on Titanium Diboride Ceramic material with various Electrode materials and dielectric fluids

Karthik S[1] and **Sivakumar Annamalai**[2]

[1] Department of Aeronautical Engineering, Excel Engineering College, Komarapalayam, Tamil Nadu-637303, India
[2] Department of Mechanical Engineering, Excel Engineering College, Komarapalayam, Tamil Nadu-637303, India

E-mail: kcg.karthi@gmail.com and askmechkongu@gmail.com

Keywords: Electrical Discharge Machining, MRR, TWR, ceramic material, overcut, dielectric fluid, regression analysis

Abstract

Titanium Diboride is a highly used material in aerospace industry due of its remarkable longevity. Its strength poses a problem to traditional machining methods. This work aims to compare two different dielectric fluids and four different electrode materials to improve EDM process parameters in TiB_2 material. The input parameters were adjusted to find the optimal combination. By studying the fluctuations of output parameters such as MRR, TWR, SR and overcut when processing titanium diboride, researchers can gain valuable insights. This is achieved through experimental studies and the results are then verified using a theoretical regression model. Experimental results confirmed that discharge current, voltage and T_{on} had a remarkable influence on MRR, TWR and surface roughness in TiB_2 material. It has been observed that tool wear rate when using kerosene-based dielectric fluids is higher than that of deionized water-based dielectric fluids. Tungsten copper electrodes cause slightly less tool wear than tungsten electrodes, and produce higher MRR overall, when compared to other three electrode materials. Using deionized water as a dielectric fluid and a copper as an electrode material can help to obtain a smoother surface. When deionized water is used as a dielectric fluid with tungsten electrodes, the overcut value drops dramatically. Brass electrodes produce a higher overcut value compared to the other three electrode materials. The microstructure of the EDM hole was distinguished by SEM analysis, and the material composition of TIB_2 was determined by EDS analysis.

Nomenclature used in this article

TiB_2	Titanium diboride
EDM	Electrical Discharge Machining
MRR	Material Remove Rate
TWR	Tool Wear Rate
SR	Surface Roughness
OC	Overcut
SEM	Scanning Electron Microscope
EDS	Energy-dispersive x-ray spectroscopy
Cu	Copper
WCu	Tungsten Copper
W	Tungsten
T_{on}	Pulse on Time
T_{off}	Pulse off Time

I_p	Discharge Current
V	Gap Voltage
Adj SS	Adjusted sums of squares
Adj MS	Adjusted mean squares
F-value	Test statistic
P-value	Probability that measures evidence against the null hypothesis
DF	Degrees of Freedom

1. Introduction

Titanium diboride (TiB_2) ceramic material is utilized in a range of applications owing to its high hardness, superior electrical conductivity, good thermal stability, high strength and wear resistance at elevated temperatures. Due to its high hardness and strength, it is complicated to cut or drill utilizing traditional machining methods. The application of unconventional processing techniques is therefore suggested [1] EDM is an extensively applied non-traditional machining methods for making intricate shaped parts, especially for materials that are difficult to machine, such as titanium alloys and ceramic materials [2]. The selection of dielectric fluid and electrode material are critical factors that affect the overall performance of the EDM process [3]. Deionized water and kerosene are frequently applied as dielectric fluids in the electrical discharge machining (EDM) of titanium alloys. Deionized water possesses outstanding insulating characteristics and can improve the effectiveness of material removal rate, whilst kerosene provides great flushing capabilities and can lead to improved surface finish [4]. The Ti-5Al-2.5Sn titanium alloy workpiece was developed by Bhaumik *et al* machined by spark erosion EDM [5] for determining the surface roughness and the overcut effect of copper, zinc and brass electrodes. Wang *et al* [6] investigated the influence of dielectric fluid properties on the EDM of titanium alloys and evolved an recent composite dielectric that accomplished better performance than distilled water and kerosene with reference to MRR, electrode wear ratio and surface roughness. Torres *et al* [7] used titanium diboride material in electric discharge machining with copper electrode to analyze the influence of surface roughness by varying discharge current, pulse on time and duty factor. Muhammad Umar Farooq *et al* [8] compared the dielectric fluid mixed with nonionic fluids with the kerosene dielectric fluids using cryogenically treated aluminum electrode when machining titanium alloys (Ti6Al4V) [9]. The experimental results show that dielectric fluids mixed with nonionic fluids had fewer machining errors and a lower wear rate, but the material removal rate was significantly the same as kerosene dielectric fluids. Ramasubbu *et al* [10] studied coconut oil, kerosene, and silicon -copper powder mixed kerosene based dielectric fluid in EDM using Hastelloy B2 material and found that coconut oil based dielectric fluids in EDM increased MRR, better surface quality and less electrode wear when compared to other two dielectric fluids. Baroi *et al* [11] studied the performance of titanium alloys in electrical discharge machining using dielectric fluid based on deionized water and copper as electrode material and discussed the importance of deionized water as a replacement for hydrocarbon oils, which pose serious hazards to human health. Perumal *et al* [12] analyzed the Ti-6Al-2Sn-4Zr-2Mo material in EDM using an orthogonal Taguchi array and found that the main influencing parameters are V, I_p and T_{on}. Shabarinathan *et al* [13] developed a copper and aluminum graphite electrode and analyzed the MRR and TWR in the Inconel alloy. The composite tool electrode gave a better MRR than the copper tool electrode because the thermal conductivity of the material increased due to the addition of graphite particles in the aluminum. The addition of biosilica particle in deionized water dielectric fluids increase the machining performance such as MRR of titanium alloy Ti-6Al-4 V in electric discharge process, TWR rate is also decreased due to addition of biosilica particles in dielectric fluids [14]. Rakshaskar *et al* [15] study the EDM of Ti-6Al-4V with aluminum electrodes fabricated using various fabrication techniques such as casting, extrusion, and 3D printing. Conventional oil dielectric fluids and lemon peel-based biodiesel dielectric fluids are used as dielectrics in the processing experiments. When comparing three process electrodes, the electrode made by casting method achieves better MRR, But SR and TWR are better in 3D printed electrode material. Satija *et al* [16] used the EDM process on a titanium alloy with a copper- tungsten electrode to investigate MRR, TWR and surface finish considering Ip, peak duration and T_{off}. The TWR is higher for copper electrodes than for tungsten copper electrodes because the addition of tungsten to copper reduces the TWR. The MRR removal rate is almost the same as copper electrodes. Sawant [17] examined the effect of several electrode materials, Cu, WCu and W, as well as different process parameters. The highest MRR is attained for the WCu electrode with the lowest tool wear rate because the Cu electrode generates a higher TWR owing to the high thermal conductivity. Darji *et al* [18] studied EN-31 material with aluminum as tool electrode in EDM and the output parameters were predicted using regression models. ANOVA was used to detect the most important input parameter. Carbon nanotubes

Figure 1. EDM machine.

Table 1. Properties of titanium diboride material.

Physical properties							
Property	Density	Melting point [7]	Specific heat [7]	Hardness (Vicker)	Young's modulus	Poisson's ratio	Thermal conductivity
Value	4.420 g.cm^3	5378 °F	870 J kg^{-1}- K^{-1}	25–35 GPa	560–600 Gpa	0.11	25 W m.K^{-1}

Chemical composition			
Titanium	Boron	Silicon	Carbon
63.93	27.49	4.00	4.57

combined with dielectric fluid improve the surface roughness of the processed material. The literature review confirmed that few studies have been conducted on titanium diboride material using deionized water as dielectric fluid and copper as electrode material to determine MRR, TWR and surface roughness. However, no studies have been conducted by means of kerosene as a dielectric fluid and tungsten copper, brass, tungsten copper and tungsten as an electrode in titanium diboride material. Therefore, current research focused on processing titanium diboride material using kerosene and deionized water as dielectric fluid and copper, brass, tungsten copper and tungsten as electrode material, considering T_{on}, T_{off}, voltage and I_p as input process parameters to determine MRR , SR TWR and overcut.

2. Materials and methods

2.1. Selection of workpiece

The workpiece is made of titanium diboride ceramic material sourced from DOMADIA Private Limited, India and has dimensions of 120 mm × 120 mm × 10 mm. The features of the titanium diboride material are shown in table 1. Due to its exceptional properties, including high hardness and wear resistance at high temperatures, titanium diboride is suitable for a variety of industries [1].

2.2. Equipment and materials

EDM drilling machining is shown in figure 1, which is used to drill small holes in TiB_2 material. The work table size of the EDM machine is 310 × 486 mm and the table can move 300 mm × 400 mm. Electrodes with a

Figure 2. TiB_2 workpiece with EDM hole.

Table 2. Input process parameters and its level.

Input parameters	Unit	Range	Levels			
			1	2	3	4
Pulse on Time (T_{on})	µs	5–20	5	10	15	20
Discharge Current (I_p)	A	2–8	2	4	6	8
Pulse off Time (T_{off})	µs	10–40	10	20	30	40
Gap Voltage (V)	V	30–60	30	40	50	60

Table 3. Properties of electrode materials.

Properties of electrode	Density (kg/m^3)	Melting temperature (°C)	Hardness (HV)	Specific heat capacity (J/(gK)	Thermal conductivity (W/mk)
Cu	896	1080	45–150	0.386	410
Brass	8733	850–950	50–185	0.383	163
W	19300	3410	410-430	0.134	175
W Cu	16745	1300–1700	110–265	0.331	235

diameter of 0.3 mm to 3 mm can be used and we can drill holes up to a maximum depth of 300 mm with drill EDM. The dielectric fluid water tank capacity is 30 liters. Deionized water, water, saponification and kerosene can be used as the dielectric liquid. An electric motor is used to move the electrode in the *Z* axis up to 320 mm. In our study, we chose electrode rods made of brass, copper, tungsten copper and tungsten with a diameter of 3 mm, with which holes were drilled into the titanium diboride material. The electrode material is selected according to their melting point, hardness, thermal, electrical conductivity [5]. A total of 64 holes were drilled with EDM, 16 each with brass, Cu, W and CuW electrodes, as shown in figure 2. Both workpiece and electrode weights were measured before and after each experiment. The four input parameters with four levels are listed in table 2. The choice of input parameters depends on the capacity of the EDM machine and on the basis of existing literature. The working time for each test with different input parameters was noted.

In table 3, we can see the characteristics of various electrode materials [1, 10, 12, 14]. The characteristics of the electrode materials evaluate the machine surface quality, MRR, TWR. The electrode material is crucial in determining the overall efficiency of the EDM process.

2.3. Dielectric fluid

When deciding on the appropriate dielectric fluid for EDM, several factors must be considered. These include the nature of the material being processed, the desired level of precision, welfare concerns and the impact on the environment. Each fluid has its own advantages and disadvantages that determine its suitability for different EDM applications. Deionized water is a non-toxic and environmentally friendly liquid that has high dielectric strength, prevents unwanted discharges due to its low conductivity, and has good cooling properties due to its high thermal conductivity [7]. Kerosene has moderate dielectric strength, a lower evaporation rate compared to deionized water, poses a lower risk of corrosion compared to deionized water, and its good lubricating properties make it suitable for machining complicated geometries [6].

3. Experimental result

The experimental result of EDM in titanium diboride material using different electrodes and dielectric fluids is shown in tables 4 and 5. The input process parameters selected for this study are T_{on}, gap voltage, T_{off}, I_p and the dependent variable is MRR, SR, overcut, TWR.

4. Regression model

Regression analysis is a mathematical tool for determining influences between the continuous predictor variables T_{on}, T_{off}, V, I_p and the response variables MRR, TWR, SR and Overcut. The machining errors obtained based on the different input parameters are determined using the regression model [8]. During model selection, interaction by order and terms by order are set to 2. For all intervals, the confidence level is set to 95%, the confidence type is selected as two-sided, type 3 is selected for sum of squares tests, and no Box–Cox transformation is selected during the analysis. The higher R^2 value indicates that the results fit the model better [8]. Tables 6–13 show the regression analysis of TiB_2 material using two different dielectric fluids and four different electrode materials. The R^2 value of all models is above 85%, which indicates that the model is almost perfect and the error percentage is also less, as shown in tables 6–13. Equations (1) to (16) show the regression model for deionized water, and equations (17) to (32) show the regression model for MRR, TWR, SR, Overcut against various predictor variables for kerosene dielectric fluid. The predicted theoretical value of regression model is shown in tables 14 and 15. In the regression model, the strength of surface roughness and overcut is lower due to the lower R^2 &R^2(adj) value, while MRR and TWR fit the regression model perfectly due to the higher R^2 &R^2(adj) value [18].

$$\mathrm{MRR}_{Copper} = -0.610 + 0.10845\ \mathrm{T_{on}} + 0.01217\ \mathrm{T_{off}} + 0.0291\ \mathrm{I_p} - 0.00072\ \mathrm{V} \tag{1}$$

$$\mathrm{MRR}_{\mathrm{Brass}} = -0.2657 + 0.05452\ \mathrm{T_{on}} + 0.00699\ \mathrm{T_{off}} - 0.00736\ \mathrm{I_p} - 0.00133\ \mathrm{V} \tag{2}$$

$$\mathrm{MRR}_{\mathrm{Tungsten\ copper}} = -0.712 + 0.15364\ \mathrm{T_{on}} + 0.01647\ \mathrm{T_{off}} - 0.0044\ \mathrm{I_p} - 0.00017\ \mathrm{V} \tag{3}$$

$$\mathrm{MRR}_{\mathrm{Tungsten}} = -0.1797 + 0.04777\ \mathrm{T_{on}} + 0.005400\ \mathrm{T_{off}} + 0.00345\mathrm{I_p} - 0.002285\ \mathrm{V} \tag{4}$$

$$\mathrm{TWR}_{\mathrm{Copper}} = -0.423 + 0.0598\ \mathrm{T_{on}} + 0.00829\ \mathrm{T_{off}} + 0.0021\ \mathrm{I_p} - 0.00005\ \mathrm{V} \tag{5}$$

$$TWR_{Brass} = -0.1885 + 0.03576\ T_{on} + 0.00495\ T_{off} - 0.01065\ I_p - 0.00014\ V \tag{6}$$

$$TWR_{Tungsten\ copper} = -0.1020 + 0.02083\ T_{on} + 0.002965\ T_{off} + 0.00450\ I_p + 0.001295\ V \tag{7}$$

$$TWR_{Tungsten} = -0.089 + 0.0120\ T_{on} + 0.00510\ T_{off} + 0.0102\ I_p + 0.00180\ V \tag{8}$$

$$SR_{Copper} = 1.27 + 0.0472\ T_{on} + 0.0368\ T_{off} - 0.0098\ I_p + 0.0068\ V \tag{9}$$

$$SR_{Brass} = 1.416 + 0.1062\ T_{on} + 0.0020\ T_{off} + 0.0544\ I_p - 0.0037\ V \tag{10}$$

$$SR_{Tungsten\ copper} = 0.866 + 0.0698\ T_{on} + 0.0212\ T_{off} - 0.0021\ I_p + 0.0203\ V \tag{11}$$

$$SR_{Tungsten} = 4.828 + 0.01215\ T_{on} + 0.01926\ T_{off} - 0.1289\ I_p - 0.01036\ V \tag{12}$$

$$OC_{Copper} = -0.012 + 0.00450\ T_{on} - 0.00090\ T_{off} + 0.0150\ I_p + 0.00115\ V \tag{13}$$

$$OC_{Brass} = 0.2095 + 0.00090\ T_{on} - 0.00010\ T_{off} - 0.00800\ I_p - 0.00160\ V \tag{14}$$

$$OC_{Tungsten\ copper} = -0.0214 + 0.00155\ T_{on} - 0.00022\ T_{off} + 0.00813\ I_p + 0.00172\ V \tag{15}$$

$$OC_{Tungsten} = 0.3335 - 0.00380\ T_{on} - 0.00065\ T_{off} - 0.00650\ I_p - 0.00230\ V \tag{16}$$

$$MRR_{Copper} = -0.659 + 0.11712\ T_{on} + 0.01314\ T_{off} + 0.0315\ I_p - 0.00078\ V \tag{17}$$

$$MRR_{Brass} = -0.2843 + 0.05833\ T_{on} + 0.00748\ T_{off} - 0.00788\ I_p - 0.00143\ V \tag{18}$$

$$MRR_{Tungsten\ copper} = -0.769 + 0.16594\ T_{on} + 0.01778\ T_{off} - 0.0048\ I_p - 0.00018\ V \tag{19}$$

$$MRR_{Tungsten} = -0.1958 + 0.05207\ T_{on} + 0.005886\ T_{off} + 0.00376\ I_p - 0.002491\ V \tag{20}$$

$$TWR_{Copper} = -0.318 + 0.04485\ T_{on} + 0.00622\ T_{off} + 0.0016\ I_p - 0.00004\ V \tag{21}$$

$$TWR_{Brass} = -0.1300 + 0.02467\ T_{on} + 0.003416\ T_{off} - 0.00735\ I_p - 0.000097\ V \tag{22}$$

$$TWR_{Tungstencopper} = -0.0571 + 0.011665\ T_{on} + 0.001660\ T_{off} + 0.00252\ I_p + 0.000725\ V \tag{23}$$

$$TWR_{Tungsten} = -0.041 + 0.00552\ T_{on} + 0.00235\ T_{off} + 0.0047\ I_p + 0.00083\ V \tag{24}$$

$$SR_{Copper} = 1.42 + 0.0529\ T_{on} + 0.0413\ T_{off} - 0.011\ I_p + 0.0076\ V \tag{25}$$

Table 4. Experimental result- deionized water dielectric fluid.

S. no.	Experimental result- deionized water dielectric fluid																			
	Input parameters				Copper electrode				Brass electrode				Tungsten copper electrode				Tungsten electrode			
	T_{on} (µs)	T_{off} (µs)	I_p (A)	V (v)	MRR (mm^3/min)	TWR (mm^3/min)	SR (µm)	Overcut (mm)	MRR (mm^3/min)	TWR (mm^3/min)	SR (µm)	Overcut (mm)	MRR (mm^3/min)	TWR (mm^3/min)	SR (µm)	Overcut (mm)	MRR (mm^3/min)	TWR (mm^3/min)	SR (µm)	Overcut (mm)
1	5	10	2	30	0.095	0.138	2.179	0.062	0.021	0.123	1.898	0.158	0.214	0.105	2.010	0.051	0.058	0.094	4.488	0.215
2	5	20	4	40	0.796	0.339	2.660	0.105	0.338	0.212	2.752	0.129	1.145	0.211	2.260	0.069	0.368	0.216	4.302	0.180
3	5	30	6	50	1.426	0.729	3.298	0.145	0.696	0.416	3.385	0.130	2.100	0.099	3.120	0.099	0.589	0.312	4.005	0.150
4	5	40	8	60	2.256	1.115	4.000	0.185	1.019	0.515	4.000	0.110	2.999	0.489	3.420	0.126	0.991	0.476	4.100	0.101
5	10	10	4	50	0.215	0.042	2.125	0.075	0.069	0.058	2.102	0.128	0.398	0.111	2.568	0.071	0.089	0.153	4.232	0.185
6	10	20	2	60	0.698	0.242	2.521	0.125	0.289	0.165	2.795	0.112	1.008	0.200	2.740	0.091	0.275	0.179	4.531	0.180
7	10	30	8	30	1.496	0.712	3.156	0.179	0.598	0.415	3.112	0.100	2.000	0.389	3.156	0.115	0.599	0.352	4.155	0.135
8	10	40	6	40	2.125	1.108	3.660	0.202	0.970	0.598	3.845	0.105	3.110	0.535	3.878	0.125	0.899	0.512	4.487	0.095
9	15	10	6	60	0.315	0.123	2.999	0.076	0.129	0.120	2.121	0.110	0.565	0.172	2.996	0.089	0.115	0.225	3.743	0.040
10	15	20	8	50	0.799	0.339	2.890	0.142	0.326	0.200	2.415	0.112	1.138	0.269	2.986	0.110	0.329	0.256	3.954	0.152
11	15	30	2	40	0.985	0.596	2.440	0.192	0.545	0.316	3.100	0.089	1.816	0.311	3.235	0.142	0.516	0.299	3.999	0.123
12	15	40	4	30	2.165	1.109	4.230	0.220	0.999	0.610	3.670	0.086	3.129	0.512	4.285	0.147	0.898	0.512	4.296	0.070
13	20	10	8	40	0.436	0.218	3.425	0.076	0.196	0.139	1.919	0.099	0.712	0.217	3.124	0.099	0.152	0.316	4.106	0.141
14	20	20	6	30	0.899	0.439	3.260	0.129	0.395	0.278	2.434	0.089	1.392	0.312	3.330	0.112	0.317	0.312	4.412	0.110
15	20	30	4	60	1.498	0.598	3.163	0.200	0.598	0.378	3.119	0.072	1.916	0.382	3.562	0.150	0.516	0.341	4.012	0.080
16	20	40	2	50	1.962	0.886	2.856	0.249	0.795	0.442	3.915	0.065	2.512	0.428	3.875	0.181	0.735	0.380	3.519	0.062

Table 5. Experimental result- kerosene dielectric fluid.

S. no.	Experimental result- kerosene dielectric fluid																			
	Input parameters				Copper electrode				Brass electrode				Tungsten copper electrode				Tungsten electrode			
	T_{on} (μs)	T_{off} (μs)	I_p (A)	V (v)	MRR (mm^3/min)	TWR (mm^3/min)	SR (μm)	Overcut (mm)	MRR (mm^3/min)	TWR (mm^3/min)	SR (μm)	Overcut (mm)	MRR (mm^3/min)	TWR (mm^3/min)	SR (μm)	Overcut (mm)	MRR (mm^3/min)	TWR (mm^3/min)	SR (μm)	Overcut (mm)
1	5	10	2	30	0.103	0.129	2.440	0.007	0.022	0.109	2.107	0.017	0.231	0.100	2.171	0.006	0.057	0.099	4.398	0.024
2	5	20	4	40	0.860	0.139	2.979	0.012	0.060	0.129	2.293	0.013	0.398	0.179	2.667	0.009	0.099	0.102	4.216	0.020
3	5	30	6	50	1.540	0.128	3.330	0.016	0.125	0.145	2.412	0.009	0.598	0.109	3.682	0.012	0.145	0.135	3.925	0.017
4	5	40	8	60	2.436	0.172	3.719	0.020	0.150	0.160	2.516	0.005	0.716	0.125	4.036	0.015	0.185	0.175	4.018	0.011
5	10	10	4	50	0.232	0.200	2.725	0.014	0.260	0.198	2.715	0.015	1.098	0.111	3.030	0.013	0.298	0.089	4.147	0.017
6	10	20	2	60	0.754	0.226	3.119	0.014	0.332	0.152	2.678	0.012	1.222	0.145	3.456	0.011	0.300	0.111	4.440	0.013
7	10	30	8	30	1.616	0.339	3.398	0.020	0.452	0.165	3.212	0.011	1.412	0.145	3.425	0.013	0.499	0.159	4.072	0.017
8	10	40	6	40	2.295	0.369	3.800	0.015	0.435	0.210	3.098	0.012	1.621	0.178	3.875	0.012	0.489	0.179	4.397	0.014
9	15	10	6	60	0.340	0.412	3.117	0.021	0.540	0.220	3.568	0.058	1.912	0.189	3.689	0.016	0.516	0.136	3.668	0.009
10	15	20	8	50	0.863	0.480	3.237	0.021	0.638	0.256	3.512	0.007	2.121	0.229	3.995	0.018	0.526	0.158	3.875	0.012
11	15	30	2	40	1.064	0.498	3.635	0.013	0.736	0.332	3.441	0.014	2.200	0.212	3.817	0.009	0.612	0.138	3.919	0.016
12	15	40	4	30	2.338	0.656	4.125	0.014	0.819	0.356	3.689	0.016	2.512	0.226	3.999	0.008	0.698	0.189	4.210	0.016
13	20	10	8	40	0.471	0.600	3.128	0.024	0.890	0.339	4.112	0.011	2.712	0.246	3.686	0.015	0.811	0.159	4.024	0.013
14	20	20	6	30	0.971	0.698	3.468	0.019	0.998	0.398	4.216	0.012	2.852	0.258	3.929	0.013	0.929	0.168	4.324	0.014
15	20	30	4	60	1.618	0.700	4.100	0.022	0.999	0.451	3.562	0.010	3.110	0.280	4.652	0.017	0.851	0.192	3.932	0.009
16	20	40	2	50	2.119	0.798	4.565	0.015	1.120	0.496	3.815	0.013	3.128	0.292	4.573	0.020	0.956	0.200	4.216	0.010

Table 6. MRR regression model for deionized water.

Source	DF	Dielectric fluid—deionized water															
		Copper electrode				Brass electrode				Tungsten copper electrode				Tungsten electrode			
		Adj SS	**Adj MS**	**F- Value**	**P- Value**	**Adj SS**	**Adj MS**	**F- Value**	**P- Value**	**Adj SS**	**Adj MS**	**F- Value**	**P- Value**	**Adj SS**	**Adj MS**	**F- Val ue**	**P- Val ue**
T_{on}	1	5.88043	5.88043	159.84	0.000	1.48594	1.48594	720.82	0.000	5.88043	5.88043	159.84	0.000	1.14099	1.14099	751.6	0.000
T_{off}	1	0.29604	0.29604	8.05	0.016	0.09779	0.09779	47.44	0.000	0.29604	0.29604	8.05	0.016	0.05832	0.05832	38.39	0.000
I_p	1	0.06789	0.06789	1.85	0.202	0.00434	0.00434	2.10	0.175	0.06789	0.06789	1.85	0.202	0.00095	0.00095	0.63	0.445
V	1	0.00104	0.00104	0.03	0.870	0.00355	0.00355	1.72	0.216	0.00104	0.00104	0.03	0.870	0.01044	0.01044	6.87	0.024
Error	11	0.40469	0.03679			0.02268	0.00206			0.40469	0.03679			0.01671	0.00152		
Total	15	6.65009	$R^2 = 93.91\%$,$R^2(adj) = 91.70\%$,$R^2(Pre) = 88.86\%$			1.61430	$R^2 = 98.60\%$,$R^2(adj) = 98.08\%$,$R^2(Pre) = 96.80\%$			6.65009	$R^2 = 99.02\%$,$R^2(adj) = 98.67\%$,$R^2(Pre) = 97.91\%$			1.22741	$R^2 = 99.02\%$,$R^2(adj) = 98.67\%$,$R^2(Pre) = 97.91\%$		

Table 7. TWR regression model for deionized water.

Source	DF	Dielectric fluid—deionized water															
		Copper electrode				Brass electrode				Tungsten copper electrode				Tungsten electrode			
		Adj SS	**Adj MS**	**F- Value**	**P- Value**	**Adj SS**	**Adj MS**	**F- Value**	**P- Value**	**Adj SS**	**Adj MS**	**F- Value**	**P- Valu e**	**Adj SS**	**Adj MS**	**F- Value**	**P- Value**
T_{on}	1	1.78799	1.78799	26.26	0.000	0.63938	0.63938	183.26	0.000	0.21694	0.21694	251.67	0.000	0.072120	0.072120	1.33	0.274
T_{off}	1	0.13761	0.13761	2.02	0.183	0.04900	0.04900	14.05	0.003	0.01758	0.01758	20.40	0.001	0.052020	0.052020	0.96	0.349
I_p	1	0.00034	0.00034	0.01	0.945	0.00907	0.00907	2.60	0.135	0.00162	0.00162	1.88	0.198	0.008364	0.008364	0.15	0.702
V	1	0.00000	0.00000	0.00	0.993	0.00003	0.00003	0.01	0.917	0.00335	0.00335	3.89	0.074	0.006480	0.006480	0.12	0.736
Error	11	0.74895	0.06809			0.03837	0.00348			0.00948	0.00086			0.598198	0.054382		
Total	15	2.67489	$R^2 = 94.78\%, R^2(adj) = 92.89\%, R^2(Pre) = 87.51\%$			0.73588	$R^2 = 98.60\%, R^2(adj) = 98.08\%, R^2(Pre) = 96.80\%$			0.24898	$R^2 = 96.19\%, R^2(adj) = 94.81\%, R^2(Pre) = 91.76\%$			0.737182	$R^2 = 95.02\%, R^2(adj) = 95.67\%, R^2(Pre) = 93.91\%$		

Table 8. SR regression model for deionized water.

Source	DF	Dielectric fluid—deionized water															
		Copper electrode				Brass electrode				Tungsten copper electrode				Tungsten electrode			
		Adj SS	**Adj MS**	**F- Valu e**	**P- Value**	**Adj SS**	**Adj MS**	**F- Valu e**	**P- Value**	**Adj SS**	**Adj MS**	**F- Valu e**	**P- Value**	**Adj SS**	**Adj MS**	**F- Valu e**	**P- Value**
T_{on}	1	1.1134	1.11345	1.43	0.257	5.64453	5.64453	17.73	0.001	2.43253	2.43253	10.57	0.008	0.07375	0.07375	4.67	0.054
T_{off}	1	2.7151	2.71511	3.49	0.089	0.00780	0.00780	0.02	0.878	0.90100	0.90100	3.91	0.073	0.74206	0.74206	47.01	0.000
I_p	1	0.0076	0.00764	0.01	0.923	0.23653	0.23653	0.74	0.407	0.00036	0.00036	0.00	0.969	1.32847	1.32847	84.17	0.000
V	1	0.0923	0.09234	0.12	0.737	0.02775	0.02775	0.09	0.773	0.82215	0.82215	3.57	0.085	0.21462	0.21462	13.60	0.004
Error	11	8.5619	0.77835			3.50183	0.31835			2.53225	0.23020			0.17362	0.01578		
Total	15	12.4904	$R^2 = 92.02\%, R^2(adj) = 93.57\%, R^2(Pre) = 90.91\%$			9.41844	$R^2 = 90.02\%, R^2(adj) = 91.39\%, R^2(Pre) = 88.77\%$			6.68829	$R^2 = 93.14\%, R^2(adj) = 90.65\%, R^2(Pre) = 84.40\%$			2.53	$R^2 = 93.44\%, R^2(adj) = 91.55, R^2(Pre) = 91.40\%$		

Table 9. Overcut regression model for deionized water.

Source	DF	Dielectric fluid—deionized water															
		Copper electrode				Brass electrode				Tungsten copper electrode				Tungsten electrode			
		Adj SS	**Adj MS**	**F- Val ue**	**P- Val ue**	**Adj SS**	**Adj MS**	**F- Val ue**	**P- Val ue**	**Adj SS**	**Adj MS**	**F- Val ue**	**P- Val ue**	**Adj SS**	**Adj MS**	**F- Val ue**	**P- Val ue**
T_{on}	1	0.010123	0.010123	1.26	0.285	0.000405	0.000405	0.10	0.754	0.001201	0.001201	0.33	0.575	0.007220	0.007220	3.08	0.107
T_{off}	1	0.001619	0.001619	0.20	0.662	0.000020	0.000020	0.01	0.944	0.000101	0.000101	0.03	0.870	0.000845	0.000845	0.36	0.560
I_p	1	0.017991	0.017991	2.24	0.162	0.005120	0.005120	1.30	0.278	0.005281	0.005281	1.47	0.251	0.003380	0.003380	1.44	0.255
V	1	0.002644	0.002644	0.33	0.577	0.005120	0.005120	1.30	0.278	0.005951	0.005951	1.65	0.225	0.010580	0.010580	4.52	0.057
Error	11	0.088170	0.008015			0.043310	0.003937			0.039559	0.003596			0.025750	0.002341		
Total	15	0.120547	$R^2 = 88.86\%, R^2(adj) = 88.99\%, R^2(Pre) = 86.11\%$			.053975	$R^2 = 90.86\%, R^2(adj) = 91.19\%, R^2(Pre) = 90.21\%$			0.052094	$R^2 = 89.86\%, R^2(adj) = 90.56\%, R^2(Pre) = 89.64\%$			0.047775	$R^2 = 92.86\%, R^2(adj) = 92.88\%, R^2(Pre) = 93.64\%$		

Table 10. MRR regression model for kerosene.

Source	DF	Dielectric fluid—kerosene															
		Copper electrode				Brass electrode				Tungsten copper electrode				Tungsten electrode			
		Adj SS	**Adj MS**	**F- Value**	**P- Value**	**Adj SS**	**Adj MS**	**F- Value**	**P- Value**	**Adj SS**	**Adj MS**	**F- Value**	**P- Value**	**Ad j SS**	**Adj MS**	**F- Value**	**P- Value**
T_{on}	1	6.85893	6.85893	159.84	0.000	1.70126	1.70126	720.82	0.000	13.7675	13.7675	1066.14	0.000	1.35561	1.35561	751.16	0.000
T_{off}	1	0.34530	0.34530	8.05	0.016	0.11196	0.11196	47.44	0.000	0.6326	0.6326	48.99	0.000	0.06929	0.06929	38.39	0.000
I_p	1	0.07919	0.07919	1.85	0.202	0.00496	0.00496	2.10	0.175	0.0018	0.0018	0.14	0.713	0.00113	0.00113	0.63	0.445
V	1	0.00121	0.00121	0.03	0.870	0.00407	0.00407	1.72	0.216	0.0001	0.0001	0.01	0.945	0.01241	0.01241	6.87	0.024
Error	11	0.47203	0.04291			0.02596	0.00236			0.1420	0.0129			0.01985	0.00180		
Total	15	7.75666	$R^2 = 98.64\%, R^2(adj) = 98.14\%, R^2(Pre) = 96.92\%$			1.84821	$R^2 = 93.91\%, R^2(adj) = 91.70\%, R^2(Pre) = 88.86\%$			14.5440	$R^2 = 98.60\%, R^2(adj) = 98.08\%, R^2(Pre) = 97.91\%$			1.45829	$R^2 = 99.02\%, R^2(adj) = 98.67\%, R^2(Pre) = 96.98\%$		

Table 11. TWR regression model for kerosene.

Source	DF	Dielectric fluid—kerosene															
		Copper electrode				Brass electrode				Tungsten copper electrode				Tungsten electrode			
		Adj SS	**Adj MS**	**F- Value**	**P- Value**	**Adj SS**	**Adj MS**	**F- Value**	**P- Value**	**Adj SS**	**Adj MS**	**F- Value**	**P- Value**	**Adj SS**	**Adj MS**	**F- Value**	**P- Value**
T_{on}	1	1.00574	1.00574	26.26	0.000	0.304413	0.304413	183.26	0.000	0.068034	0.068034	251.67	0.000	0.015261	0.015261	1.33	0.274
T_{off}	1	0.07740	0.07740	2.02	0.183	0.023331	0.023331	14.05	0.003	0.005514	0.005514	20.40	0.001	0.011007	0.011007	0.96	0.349
I_p	1	0.00019	0.00019	0.01	0.945	0.004320	0.004320	2.60	0.135	0.000508	0.000508	1.88	0.198	0.001770	0.001770	0.15	0.702
V	1	0.00000	0.00000	0.00	0.993	0.000019	0.000019	0.01	0.917	0.001052	0.001052	3.89	0.074	0.001371	0.001371	0.12	0.736
Error	11	0.42128	0.03830			0.018272	0.001661			0.002974	0.000270			0.126579	0.011507		
Total	15	1.50463	$R^2 = 90.91\%, R^2(adj) = 90.99\%, R^2(Pre) = 89.86\%$			0.350355	$R^2 = 94.78\%, R^2(adj) = 92.89\%, R^2(Pre) = 87.51\%$			0.078081	$R^2 = 96.91\%, R^2(adj) = 94.81\%, R^2(Pre) = 91.76\%$			0.155988	$R^2 = 95.85\%, R^2(adj) = 94.76\%, R^2(Pre) = 94.586\%$		

Table 12. SR regression model for kerosene.

Source	DF	Dielectric fluid—kerosene															
		Copper electrode				Brass electrode				Tungsten copper electrode				Tungsten electrode			
		Adj SS	**Adj MS**	**F- Value**	**P- Value**	**Adj SS**	**Adj MS**	**F- Value**	**P- Value**	**Adj SS**	**Adj MS**	**F- Value**	**P- Value**	**Adj SS**	**Adj MS**	**F- Value**	**P- Value**
T_{on}	1	1.3967	1.39671	1.43	0.257	6.9546	6.95463	17.73	0.001	3.63975	3.63975	11.26	0.006	0.07083	0.07083	4.67	0.054
T_{off}	1	3.4058	3.40583	3.49	0.089	0.0096	0.00961	0.02	0.878	1.41012	1.41012	4.36	0.061	0.71267	0.71267	47.01	0.000
I_p	1	0.0096	0.00959	0.01	0.923	0.2914	0.29143	0.74	0.407	0.00202	0.00202	0.01	0.938	1.27586	1.27586	84.17	0.000
V	1	0.1158	0.11584	0.12	0.737	0.0342	0.03419	0.09	0.773	1.29357	1.29357	4.00	0.071	0.20612	0.20612	13.60	0.004
Error	11	10.7400	0.97636			4.3146	0.39224			3.63975	3.63975			0.16675	0.01516		
Total	15	15.6680	$R^2 = 90.81\%, R^2(adj) = 91.99\%, R^2(Pre) = 89.86\%$			11.6045	$R^2 = 92.81\%, R^2(adj) = 9.3.99\%, R^2(Pre) = 91.86\%$			9.90121	$R^2 = 88.81\%, R^2(adj) = 85.99\%, R^2(Pre) = 81.86\%$			2.43224	$R^2 = 93.14\%, R^2(adj) = 90.65\%, R^2(Pre) = 84.40\%$		

Table 13. Overcut regression model for kerosene.

Source	DF	Dielectric fluid—kerosene															
		Copper electrode				Brass electrode				Tungsten copper electrode				Tungsten electrode			
		Adj SS	**Adj MS**	**F- Value**	**P- Value**	**Adj SS**	**Adj MS**	**F- Value**	**P- Value**	**Adj SS**	**Adj MS**	**F- Value**	**P- Value**	**Adj SS**	**Adj MS**	**F- Value**	**P- Value**
T_{on}	1	0.000122	0.000122	1.26	0.285	0.000005	0.000005	0.10	0.754	0.000015	0.000015	0.33	0.575	0.000087	0.000087	3.08	0.107
T_{off}	1	0.000020	0.000020	0.20	0.662	0.000000	0.000000	0.01	0.944	0.000001	0.000001	0.03	0.870	0.000010	0.000010	0.36	0.560
I_p	1	0.000218	0.000218	2.24	0.162	0.000062	0.000062	1.30	0.278	0.000064	0.000064	1.47	0.251	0.000041	0.000041	1.44	0.255
V	1	0.000032	0.000032	0.33	0.577	0.000062	0.000062	1.30	0.278	0.000072	0.000072	1.65	0.225	0.000128	0.000128	4.52	0.057
Error	11	0.001067	0.000097			0.000524	0.000048			0.000479	0.000044			0.000312	0.000028		
Total	15	0.001459	$R^2 = 89.86\%$, $R^2(adj) = 88.99\%$, $R^2(Pre) = 86.86\%$			0.000653	$R^2 = 86.86\%$, $R^2(adj) = 84.99\%$, $R^2(Pre) = 83.86\%$			0.000630	$R^2 = 92.86\%$, $R^2(adj) = 93.49\%$, $R^2(Pre) = 90.24\%$			0.000578	$R^2 = 97.96\%$, $R^2(adj) = 98.99\%$, $R^2(Pre) = 93.13\%$		

Table 14. Theoretical result of EDM using regression model in kerosene dielectric fluid.

S. no.	Theoretical result- kerosene																			
	Input parameters				Copper electrode				Brass electrode				Tungsten copper electrode				Tungsten electrode			
	T_{on} (μs)	T_{off} (μs)	I_p (A)	V (v)	MRR (mm^3/min)	TWR (mm^3/min)	SR (μm)	Overcut (mm)	MRR (mm^3/min)	TWR (mm^3/min)	SR (μm)	Overcut (mm)	MRR (mm^3/min)	TWR (mm^3/min)	SR (μm)	Overcut (mm)	MRR (mm^3/min)	TWR (mm^3/min)	SR (μm)	Overcut (mm)
1	5	10	2	30	0.098	0.130	2.304	0.007	0.023	0.110	2.181	0.016	0.224	0.100	2.294	0.006	0.056	0.099	4.422	0.025
2	5	20	4	40	0.878	0.095	2.771	0.011	0.068	0.098	2.283	0.013	0.390	0.174	2.824	0.009	0.098	0.086	4.257	0.020
3	5	30	6	50	1.658	0.100	3.238	0.014	0.113	0.047	2.385	0.009	0.556	0.102	3.354	0.013	0.139	0.127	4.092	0.016
4	5	40	8	60	2.438	0.165	3.705	0.018	0.158	0.065	2.487	0.005	0.723	0.131	3.884	0.016	0.181	0.168	3.926	0.011
5	10	10	4	50	0.221	0.197	2.698	0.016	0.271	0.117	2.810	0.012	1.040	0.122	3.238	0.012	0.274	0.098	4.026	0.016
6	10	20	2	60	0.738	0.256	3.209	0.013	0.347	0.165	2.670	0.011	1.226	0.141	3.748	0.012	0.301	0.120	4.366	0.014
7	10	30	8	30	1.650	0.329	3.328	0.018	0.417	0.157	3.177	0.011	1.380	0.151	3.282	0.011	0.457	0.147	4.102	0.017
8	10	40	6	40	2.430	0.387	3.839	0.015	0.494	0.205	3.037	0.011	1.566	0.170	3.792	0.011	0.483	0.170	4.441	0.015
9	15	10	6	60	0.345	0.424	3.017	0.023	0.532	0.224	3.479	0.009	1.858	0.193	3.929	0.017	0.517	0.143	3.732	0.010
10	15	20	8	50	0.862	0.490	3.332	0.024	0.606	0.245	3.663	0.008	2.028	0.207	3.951	0.016	0.609	0.168	3.769	0.011
11	15	30	2	40	1.379	0.543	3.735	0.011	0.742	0.324	3.363	0.015	2.237	0.202	3.933	0.009	0.670	0.155	4.817	0.017
12	15	40	4	30	2.422	0.609	4.050	0.013	0.815	0.344	3.547	0.015	2.407	0.216	3.955	0.008	0.761	0.180	4.855	0.017
13	20	10	8	40	0.468	0.652	3.107	0.026	0.837	0.335	4.271	0.011	2.682	0.242	3.857	0.016	0.835	0.164	3.741	0.012
14	20	20	6	30	0.986	0.712	3.466	0.020	0.942	0.385	4.213	0.014	2.871	0.246	3.859	0.012	0.911	0.170	4.284	0.015
15	20	30	4	60	1.503	0.770	4.129	0.020	0.989	0.431	3.992	0.011	3.053	0.280	4.877	0.015	0.888	0.209	4.421	0.008
16	20	40	2	50	2.020	0.829	4.488	0.014	1.094	0.480	3.934	0.014	3.242	0.284	4.879	0.011	0.964	0.214	4.964	0.011

Table 15. Theoretical result of EDM using deionized water dielectric fluid medium.

S. no.	Theoretical result- deionized water																			
	Input parameters				Copper electrode				Brass electrode				Tungsten copper electrode				Tungsten electrode			
	T_{on} (μs)	T_{off} (μs)	I_p (A)	V (v)	MRR (mm^3/min)	TWR (mm^3/min)	SR (μm)	Overcut (mm)	MRR (mm^3/min)	TWR (mm^3/min)	SR (μm)	Overcut (mm)	MRR (mm^3/min)	TWR (mm^3/min)	SR (μm)	Overcut (mm)	MRR (mm^3/min)	TWR (mm^3/min)	SR (μm)	Overcut (mm)
1	5	10	2	30	0.091	0.098	2.058	0.066	0.022	0.104	1.965	0.149	0.207	0.102	2.032	0.052	0.052	0.069	4.513	0.226
2	5	20	4	40	0.813	0.348	2.643	0.110	0.350	0.221	2.625	0.137	1.131	0.222	2.589	0.074	0.351	0.228	4.508	0.188
3	5	30	6	50	1.535	0.734	3.227	0.153	0.678	0.428	3.284	0.124	2.055	0.365	3.145	0.096	0.651	0.359	4.504	0.149
4	5	40	8	60	2.257	1.120	3.812	0.197	1.006	0.635	3.944	0.112	2.979	0.508	3.702	0.117	0.951	0.491	4.499	0.111
5	10	10	4	50	0.205	0.044	2.494	0.069	0.079	0.062	1.948	0.132	0.370	0.122	2.447	0.067	0.083	0.165	4.602	0.197
6	10	20	2	60	0.684	0.264	2.343	0.130	0.267	0.170	2.568	0.122	0.965	0.206	2.580	0.093	0.274	0.195	4.212	0.171
7	10	30	8	30	1.528	0.733	3.295	0.165	0.664	0.427	3.247	0.108	2.054	0.378	3.348	0.113	0.628	0.377	4.400	0.126
8	10	40	6	40	2.250	1.119	3.880	0.208	0.992	0.634	3.907	0.096	2.978	0.521	3.905	0.135	0.928	0.509	4.396	0.088
9	15	10	6	60	0.320	0.126	2.930	0.071	0.135	0.111	1.931	0.115	0.533	0.165	2.862	0.082	0.114	0.234	4.691	0.167
10	15	20	8	50	0.798	0.347	2.779	0.133	0.323	0.219	2.551	0.105	1.128	0.248	2.995	0.108	0.306	0.264	4.301	0.142
11	15	30	2	40	1.277	0.567	2.627	0.194	0.511	0.327	3.170	0.094	1.722	0.332	3.127	0.134	0.497	0.293	3.911	0.116
12	15	40	4	30	2.243	1.119	3.948	0.220	0.979	0.633	3.870	0.080	2.976	0.534	4.108	0.152	0.905	0.527	4.292	0.065
13	20	10	8	40	0.434	0.209	3.366	0.074	0.192	0.159	1.914	0.098	0.696	0.207	3.277	0.097	0.145	0.303	4.780	0.138
14	20	20	6	30	0.913	0.429	3.215	0.135	0.380	0.267	2.534	0.088	1.291	0.291	3.410	0.123	0.337	0.333	4.390	0.112
15	20	30	4	60	1.392	0.649	3.063	0.197	0.568	0.375	3.153	0.077	1.885	0.374	3.542	0.149	0.528	0.362	4.000	0.087
16	20	40	2	50	1.870	0.870	2.912	0.258	0.756	0.483	3.773	0.067	2.480	0.458	3.675	0.176	0.720	0.392	3.611	0.061

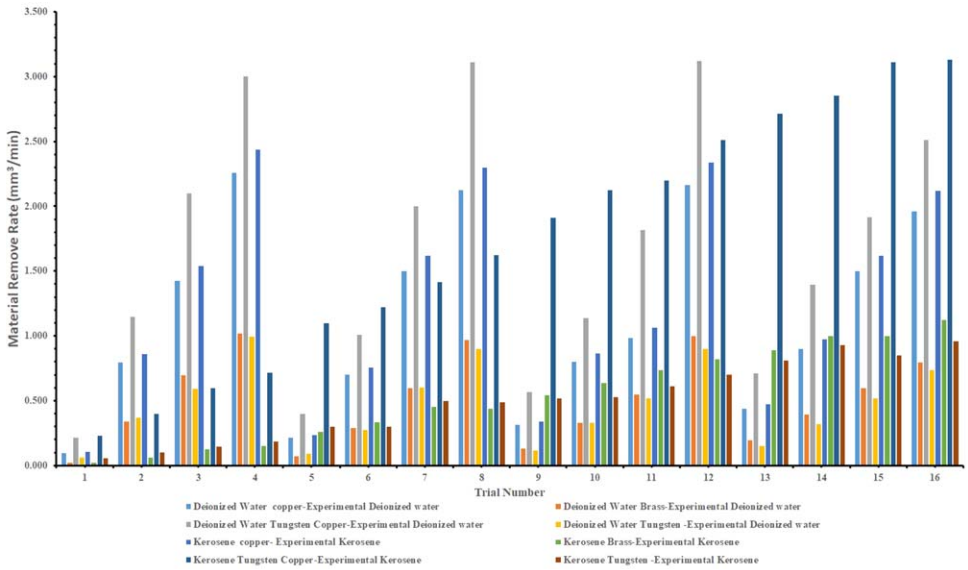

Figure 3. Material remove rate for different electrode materials and dielectric fluid.

$$SR_{Brass} = 1.572 + 0.1179\ T_{on} + 0.0022\ T_{off} + 0.0604\ I_p - 0.0041\ V \tag{26}$$

$$SR_{Tungsten\ copper} = 0.829 + 0.0853\ T_{on} + 0.0266\ T_{off} + 0.0050\ I_p + 0.0254\ V \tag{27}$$

$$SR_{Tungsten} = 4.731 + 0.01190\ T_{on} + 0.01888\ T_{off} - 0.1263\ I_p - 0.01015\ V \tag{28}$$

$$OC_{Copper} = -0.0013 + 0.000495\ T_{on} - 0.000099\ T_{off} + 0.00165\ I_p + 0.000126\ V \tag{29}$$

$$OC_{Brass} = 0.02304 + 0.000099\ T_{on} - 0.000011\ T_{off} - 0.000880\ I_p - 0.000176\ V \tag{30}$$

$$OC_{Tungsten\ copper} = -0.00235 + 0.000170\ T_{on} - 0.000025\ T_{off} + 0.000894\ I_p + 0.000190\ V \tag{31}$$

$$OC_{Tungsten} = 0.03669 - 0.000418\ T_{on} - 0.000071\ T_{off} - 0.000715\ I_p - 0.000253\ V \tag{32}$$

5. Result and discussion

5.1. Material remove rate

The material removal rate for various electrode materials and dielectric fluids is shown in figure 3. The MRR interaction diagram against four different input parameters for kerosene and deionized water is shown in figures 4(i, ii, iii, iv). The choice of dielectric fluid, input parameters and electrode material in EDM plays a crucial role in MRR. Increasing I_p from 2 A to 8 A can increase the energy input so that more energy is released per discharge current, resulting in an increase in MRR in both deionized water and dielectric kerosene fluid [17]. If we increase the T_{on} from 5 μs to 20 μs, the duration of the pulse time increases, so that the spark has enough time to interact with the sample, resulting in the formation of larger and deeper craters, so the MRR also increases due to the increase in the T_{on} value increases [1]. Selecting the correct T_{off} value ensures that the dielectric fluid cools and washes away deposits in the EDM, preventing re-solidification of the material due to subsequent discharges [19]. Increasing T_{on} value in EDM process will increase the material remove rate as shown in figure 3. Increasing the voltage from 30 V to 60 V leads to an increase in the electric field strength, which in turn leads to larger craters and higher MRR in the TiB_2 material [6]. However, due to the better viscosity of the dielectric medium, kerosene results in better MRR compared to deionized water. The electrical conductivity of copper is good. So when combined with a deionized water based dielectric fluid, it produces a MRR of 2.256 mm^3 /min when $T_{on} = 5$ μs, $T_{off} = 40$ μs, $I_p = 8$ A and V = 60 V. If we use for machining of TiB_2 using a copper electrode with a kerosene-based dielectric fluid produces a higher MRR of 2.436 mm^3 / min, which is 9% higher MRR than a water-based deionized fluid. Brass electrodes produce a lower MRR in TiB_2 compared to copper and tungsten copper electrodes due to the lower conductivity of the electrode material. The highest MRR achieved in brass electrodes using a kerosene dielectric is 1.120 mm^3 / min when $T_{on} = 20$ μs, $T_{off} = 40$ μs, $I_p = 2$ A and V = 50 V, while in a medium based on deionized water an MRR of 1.109 mm^3 / min is produced when $T_{on} = 5$ μs, $T_{off} = 40$ μs, $I_p = 8$ A and V = 60 V. Tungsten copper has high electrical and thermal conductivity. When combined with a kerosene-based dielectric medium, it produces better MRR than other three electrode materials. If we use a tungsten-copper electrode in water-based deionized liquid medium, it gives an MRR of

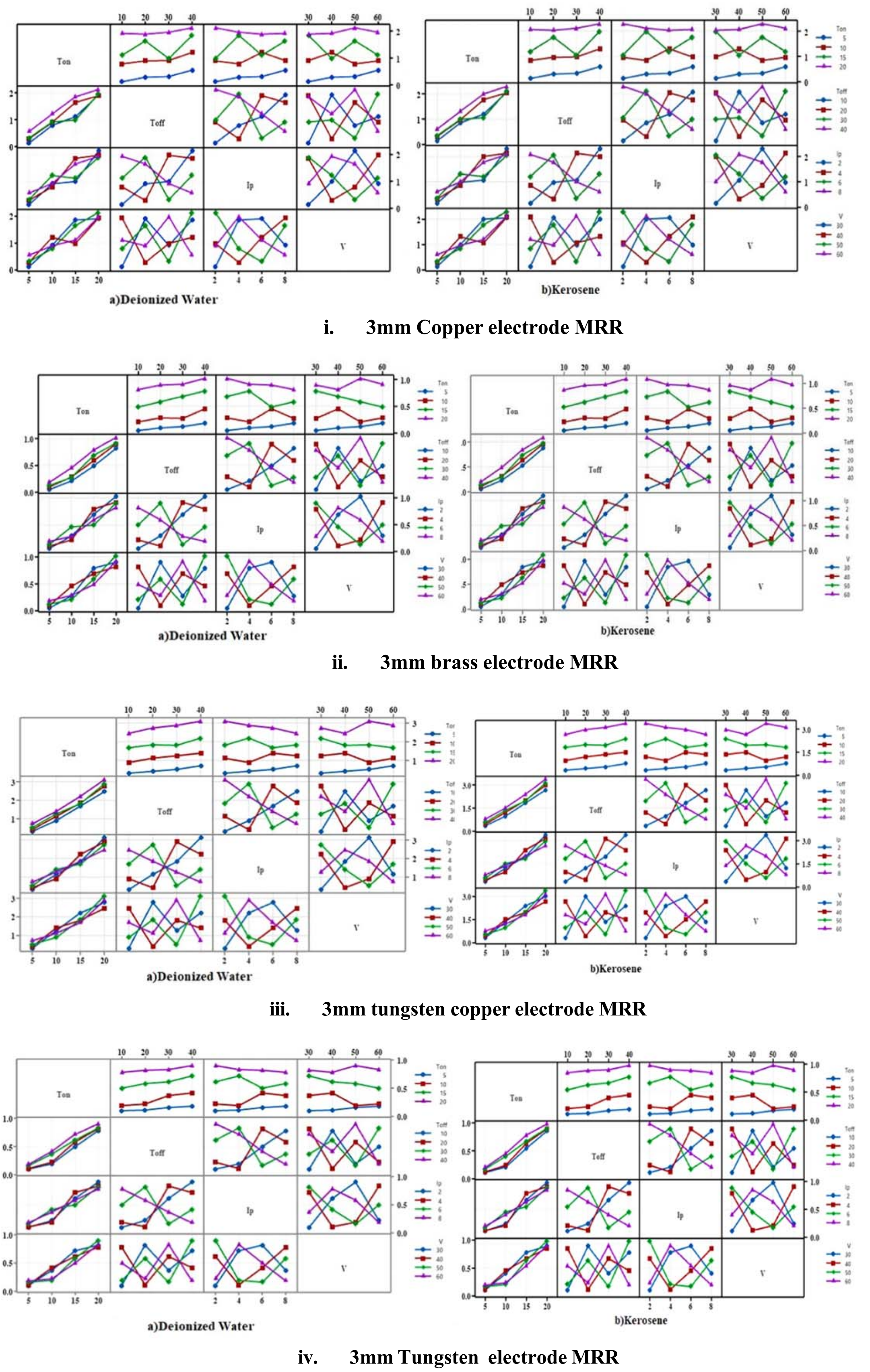

Figure 4. MRR interaction plot for different dielectric fluid and electrode materials.

3.129 mm^3 / min , if $T_{on} = 15\,\mu s$, $T_{off} = 40\,\mu s$, $I_p = 4$ A and V = 30 V. If we use a tungsten copper electrode in a dielectric kerosene liquid medium, it produces 3.128 mm^3 /min when $T_{on} = 20\,\mu s$, $T_{off} = 40\,\mu s$, $I_p = 2$ A and V = 50 V. Tungsten based electrodes have high thermal strength and high melting point, but have lower thermal

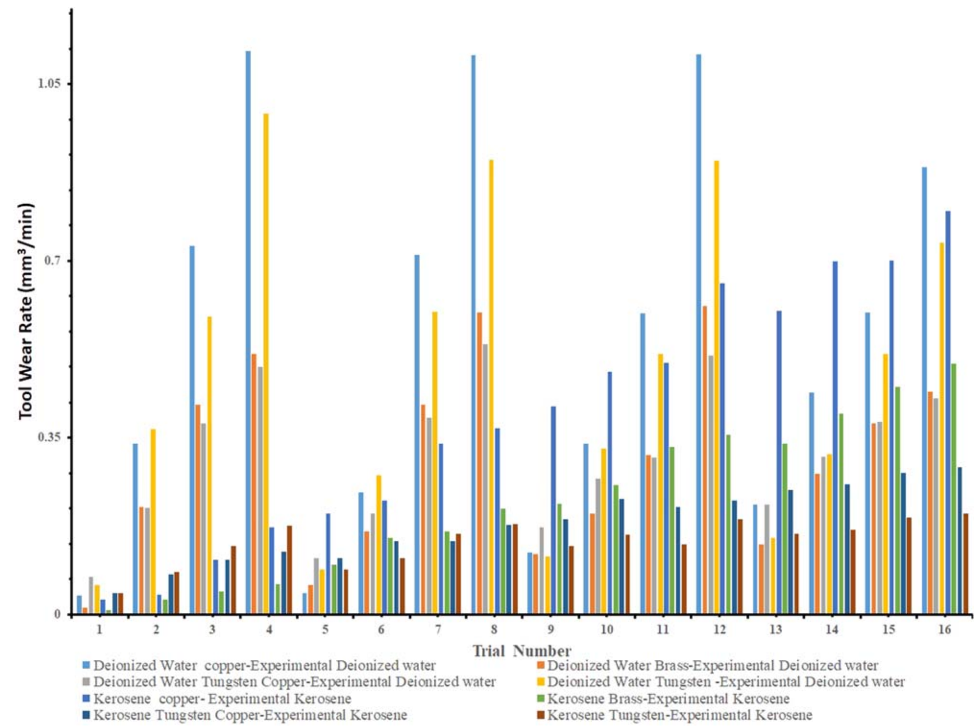

Figure 5. Tool wear rate for different electrode materials and dielectric fluid.

conductivity compared to other three electrode materials for this reason produces a lower MRR than other three electrode materials. Using a tungsten electrode in deionized water produces an MRR of 0.991 mm^3 / min when $T_{on} = 5\ \mu s$, $T_{off} = 40\ \mu s$, $I_p = 8$ A and V = 60 V, while kerosene-based dielectric fluid produces an MRR of 0.956 mm^3 / min , if $T_{on} = 20\ \mu s$, $T_{off} = 40\ \mu s$, $I_p = 2$ A and V = 50 V.

5.2. Tool wear rate

The tool wear rate for 64 experiments is shown in figure 5. The TWR interaction diagram against copper, brass, tungsten copper and tungsten electrode for kerosene and deionized water, again four different input parameters, is shown in figures 6(i, ii, iii, iv). The thermal conductivity and hardness value of titanium diboride material are high, so the heat concentrated in the workpiece during machining leads to an increase in TWR [6]. Increasing the Ip value increases the temperature in the electrode material, which also leads to increase in tool wear rate [19]. A longer pulse duration due to the increase in T_{on} and T_{off} value leads to an increase in the pulse duration and thermal stress on the electrode material, which causes an increase in TWR as shown in figure 6. The electrical conductivity of Cu and WCu electrodes is high and thus ensures the correct heat transfer during the EDM process, which reduces tool wear compared to the brass electrode. Deionized water dielectric fluids produce less TWR due to better cooling, lower electrical conductivity, and due debris washed away effectively from the workpiece [20], whereas kerosene dielectric fluids produce more TWR due to lower cooling efficiency and improved spark generation due to high electrical conductivity [21]. Based on the experiment and regression model, lower TWR is observed with 0.094 mm^3 /min for tungsten electrodes using deionized water as dielectric fluid medium when$T_{on} = 5\ \mu s$, $T_{off} = 10\ \mu s$, $I_p = 2$ A and V = 30 V. The high melting point of the tungsten electrode prevents electrode wear when machining TiB_2 material in all machining environments. If we use a tungsten copper electrode in both deionized water and kerosene medium, the lowest TWR is observed in deionized water based medium with TWR = 0.099 mm^3 / min when $T_{on} = 5\ \mu s$, $T_{off} = 30\ \mu s$, $I_p = 6$ A and V = 50 V results in a lower TWR in contrast to brass and copper electrodes, due to tool electrode high thermal conductivity allows for adequate heat dissipation during EDM. The highest TWR is observed in brass electrodes with deionized water dielectric medium with a value of TWR = 0.496 mm^3 / min when $T_{on} = 20\ \mu s$, $T_{off} = 40\ \mu s$, $I_p = 2$ A and V = 50 V, due to lower thermal conductivity, melting temperature and lower hardness compared to other three electrode materials. A copper electrode with deionized water produces a moderate TWR compared to tungsten and tungsten copper electrodes with TWR = 0.138 mm^3 / min when $T_{on} = 5\ \mu s$, $T_{off} = 10\ \mu s$, $I_p = 2$ A and V = 30 V.

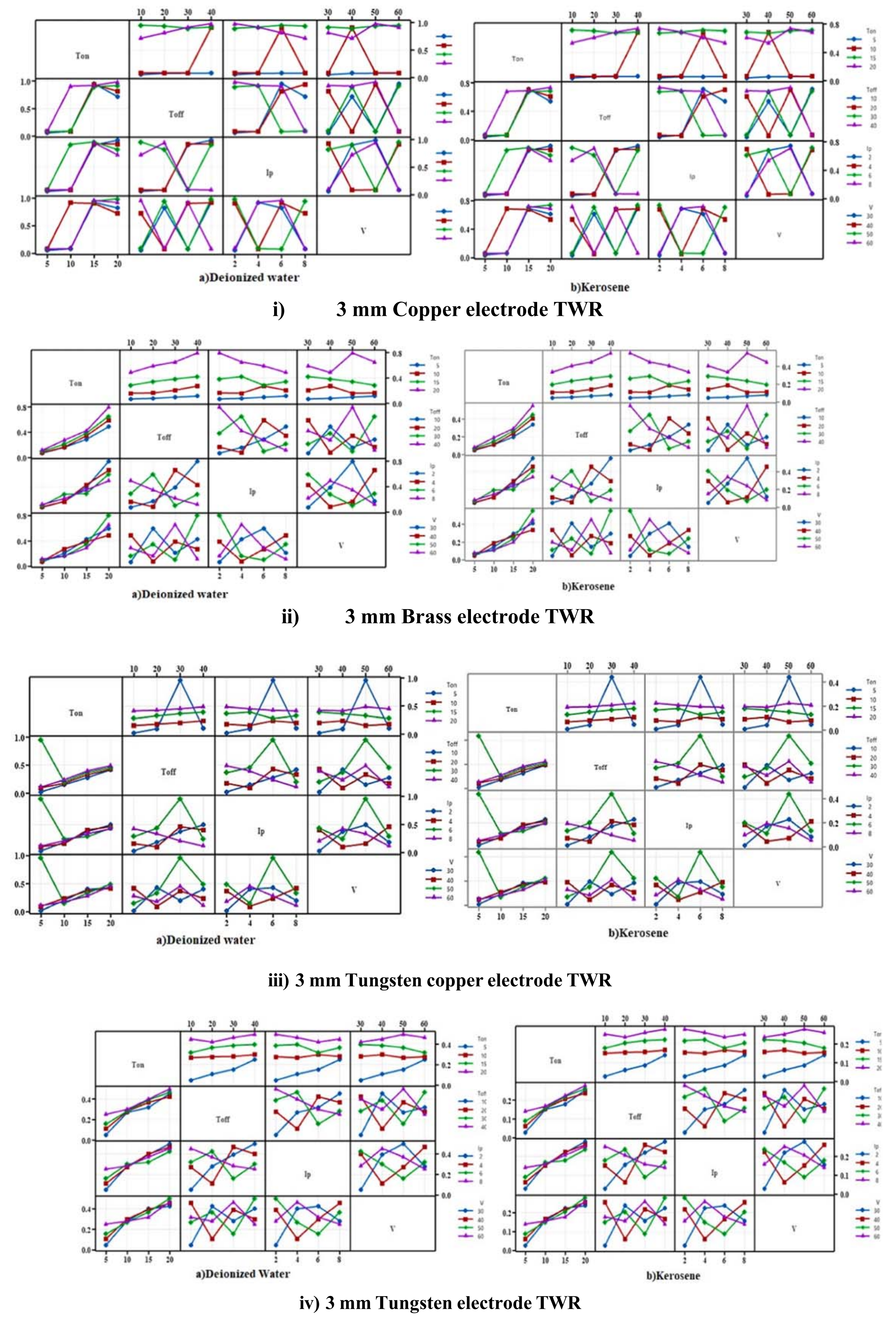

Figure 6. TWR interaction plot for different dielectric fluid and electrode materials.

5.3. Surface roughness

The mitutoyo SJ-210 surface roughness measuring device is used to measure the surface roughness of erosion holes. The surface roughness value of TiB_2 material after drilling a hole by EDM with different electrodes and dielectric fluids is shown in figures 7 and 8(i, ii, iii, iv). The surface roughness value is lower for deionized water-

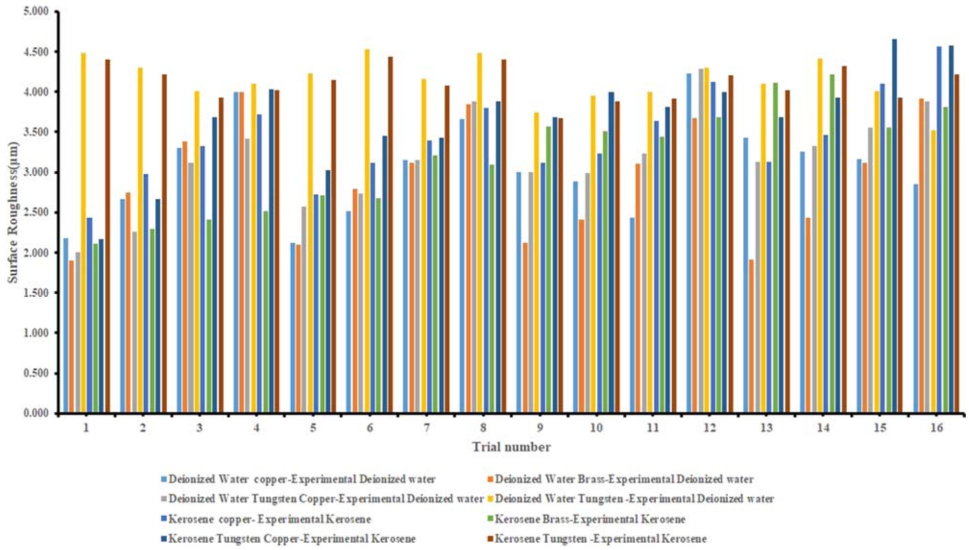

Figure 7. Surface roughness for different electrode materials and dielectric fluid.

based dielectric fluid compared to kerosene because the flushing properties and thermal conductivity of deionized water are better and enable efficient cooling, resulting in lower surface area value [21]. The copper and tungsten copper electrodes produce a good surface quality in the TiB_2 material due to the good electrical and thermal conductivity [20]. Increasing the input parameters T_{on}, T_{off}, V and I_p increases the surface roughness in the material due to a higher MRR [6, 22]. The better surface roughness value of copper electrodes using deionized water is 2.125 µm ,when $T_{on} = 10$ µs, $T_{off} = 10$ µs, $I_p = 4$ A and V = 50 V, while a better surface roughness value of 2.440 µm is observed when using kerosene-based dielectric fluid if $T_{on} = 5$ µs, $T_{off} = 10$ µs, $I_p = 2$ A and V = 30 V. The minimum surface roughness value observed for tungsten copper electrodes with kerosene is 2.107 µm, when $T_{on} = 5$ µs, $T_{off} = 10$ µs, $I_p = 2$ A and V = 30 V, whereas with deionized dielectric fluids, 1.898 µm is produced when $T_{on} = 5$ µs, $T_{off} = 10$ µs, $I_p = 2$ A and V = 30 V. The surface roughness value of the tungsten electrode can range from 3.519 µm to 4.531 µm in a dielectric medium based on deionized water, while the surface roughness value can range from 3.668 µm to 4.398 µm as in a kerosene-based dielectric fluid. Due to the higher melting point of the electrode material and good electrical conductivity, it results in a slightly rough surface finish compared to copper and tungsten copper electrodes. Brass electrodes result in poor surface finish in both dielectric fluids due to the lower melting point . The highest observed surface roughness value is 4.216 µm when $T_{on} = 20$ µs, $T_{off} = 20$ µs, $I_p = 6$ A and V = 30 V in a kerosene-based dielectric medium.

5.4. Overcut

The optical microscope and coordinate measuring machine is used to measure the diameter of the machined hole. Take several measurements at different points on the hole to confirm accuracy and account for any differences. The overcut value of different dielectric fluids, electrode materials and varying input parameters for TiB_2 material are shown in Figures 9 and 10(i, ii, iii, iv). Increasing the T_{off} values during EDM allows more time to wash away deposits between the workpiece and the electrode and more time to cool, so the area affected by the heat becomes smaller and overcut also reduced. Increasing the T_{on} value increases overcut as longer energy input results in more MRR and overcut [22]. Increasing the I_p value from 2 A to 8 A concentrates more energy at one point, resulting in more overcut and MRR. Increasing the voltage from 30 V to 60 V can increase the overcut value due to increasing the spark gap distance. Copper electrodes with dielectric on deionized water produce a moderate overcut ranging from 0.062 mm to 0.249 mm, and copper electrodes with kerosene dielectric range from 0.007 mm to 0.024 mm. Tungsten copper produces a small overcut when combined with a kerosene-based dielectric medium produces an overcut in the range of 0.006 mm to 0.020 mm, while when combined with a dielectric fluid medium based on deionized water creates an overcut of 0.051 mm to 0.181 mm. Tungsten electrodes produce less overcut due to their high wear resistance [23]. Tungsten electrode in combination with dielectric fluid on deionized water, an overcut value in the range of 0.009 mm to 0.024 mm. When combined with kerosene- based dielectric medium, the overcut values vary from 0.040 mm to 0.215 mm. Of the four electrode materials, brass electrodes produce a higher overcut value due to the high tool wear rate. The highest observed overcut value in dielectric fluid on deionized water is 0.158 mm when $T_{on} = 5$ µs, $T_{off} = 10$ µs, $I_p = 2$ A and V = 30 V, brass electrode with kerosene based dielectric fluid produces an overcut value of 0.058 mm when $T_{on} = 5$ µs, $T_{off} = 10$ µs, $I_p = 2$ A and V = 30 V.

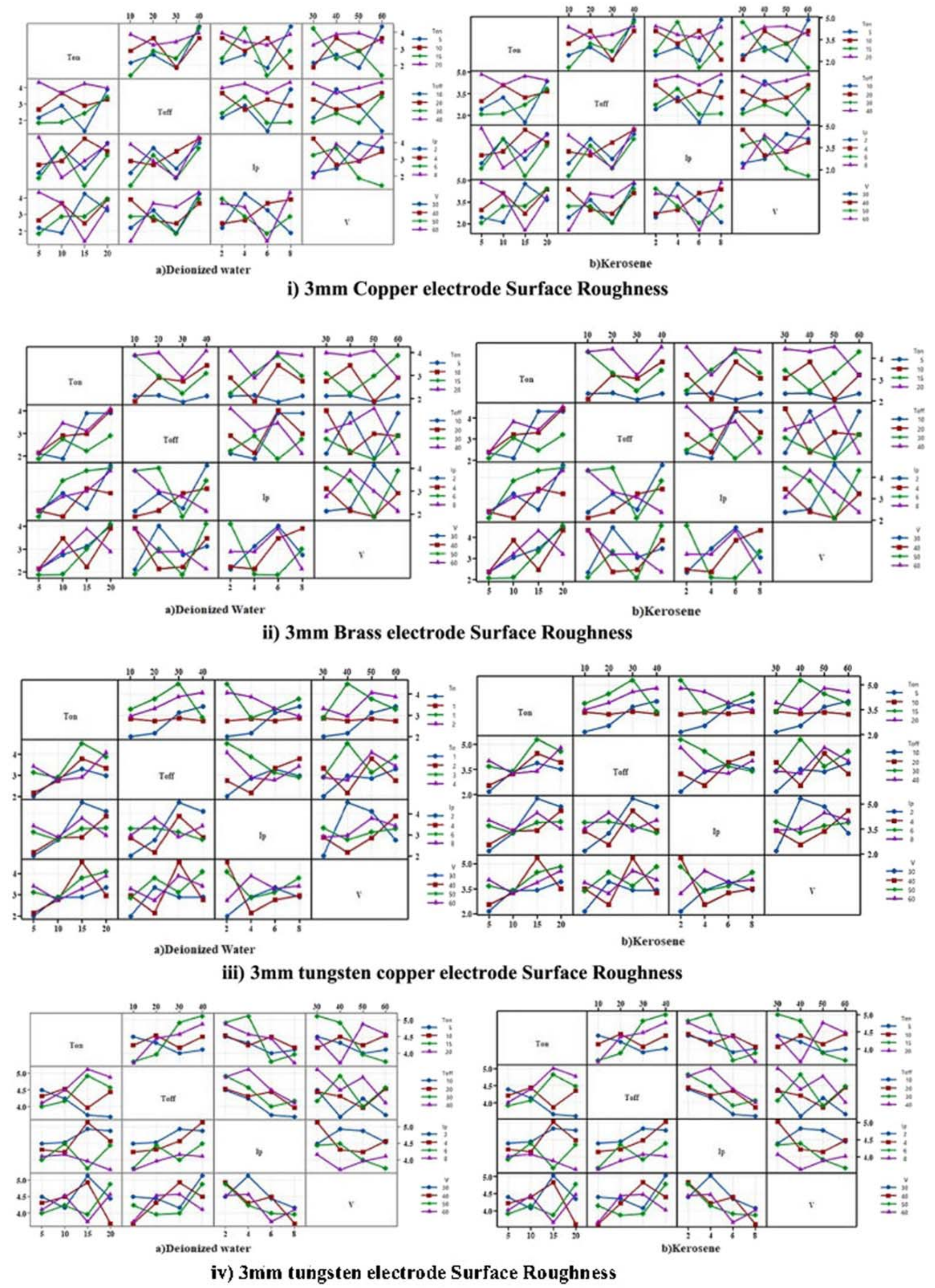

Figure 8. Surface roughness interaction plot for different dielectric fluid and electrode materials.

5.5. Material characterization

SEM tests were performed before and after drilling holes using EDM to assess the integrity, porosity and cracks of the sample surface. TiB_2 samples are prepared for SEM analysis with dimensions of 10 mm × 10 mm × 10 mm and can be cut using the DK7735 wire EDM machine. The SEM sample can be etched to improve surface contrast, remove contaminants, and reveal subsurface features and oxides present on the workpiece. This helps to increase the contrast between the different layers of the sample surface [16].

Table 16 shows the chemical composition and atomic weight percentage of the TiB_2 material determined by EDS analysis with the field emission scanning electron microscope, Carl Zeiss- Sigma 300 model. Figure 11

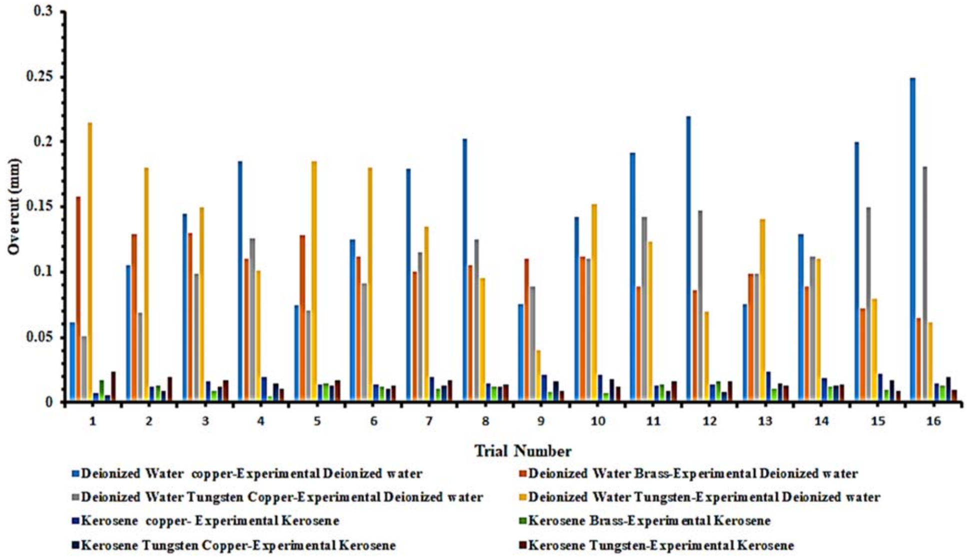

Figure 9. Overcut for different electrode materials and dielectric fluid.

Table 16. Atomic weight percentage of TiB_2 material.

Element	Weight %	Atomic %	Error %	Net Int.	R	A	F
B K	8.59	27.49	27.95	7.65	0.8232	0.0495	1.0000
C K	1.97	4.57	24.92	15.71	0.8313	0.0694	1.0000
Si K	1.00	4.00	25.99	0.17	0.8784	0.5280	1.0218
Ti K	88.44	63.93	1.97	6233.33	0.9130	0.9523	1.0127

shows SEM analysis before EDM hole drilling and figures 12(a)–(d) shows the SEM analysis after machining holes during EDM. The SEM analysis of the workpiece is carried out at a magnification of up to 1.50 KX to examine the influence of surface topography on the machined surface.

Table 16 shows the chemical composition and atomic weight percentage of the TiB_2 material determined by EDS analysis with the field emission scanning electron microscope, Carl Zeiss-Sigma 300 model. Figure 11 shows SEM analysis before EDM hole drilling and figures 12(a)–(d) shows the SEM analysis after machining holes during EDM. The SEM analysis of the workpiece is carried out at a magnification of up to 1.50 KX to examine the influence of surface topography on the machined surface. In figure 12, the tiny particles in the core of the SEM image may be a piece of dissolved grain. This could indicate the presence of tiny cracks or a deterioration in material integrity in that area. The differences in contrast and brightness between the particles and the surrounding matrix could indicate that the image represents a non-uniform material structure [24]. This can be described by variations in the composition of the materials or by the reaction of different phases to the electron beam in the SEM. Materials with higher atomic numbers, TiB_2 particles, are often represented by lighter areas, while debris or matrix areas can be represented by darker areas. There are places in the image that appear to have gaps or breaks, and there are also unevenness. This may indicate that the material has developed cracks or breaks due to heat or mechanical stress from the machining process. Figure 12(a) shows an uneven surface with visible microcracks, roughness and thermal effect of EDM on TiB_2. The high-energy electrical discharges lead to local melting and evaporation, which leads to material removal. The rapid cooling after discharge causes cracks to form due to thermal stresses [4, 24]. The cracks occur because the temperature gradients during discharge cause expansion and contraction, resulting in internal stresses that exceed the fracture toughness of the material. Figure 12(b) shows areas where molten material has resolidified after being ejected from the workpiece. This is the recast layer, a common phenomenon in EDM. Each discharge removes some of the molten material, but some of it redeposits to the surface as it solidifies. The presence of this recast layer is undesirable in precision machining because it changes the surface quality and causes defects such as inclusions and pores. In addition, it influences the electrical and mechanical properties of the processed surface. Figure 12(c) shows deep microcracks and small pits scattered across the surface. These features indicate thermal fatigue and material vaporization. Microcracks are caused by repeated temperature changes during the machining process. Pitting,

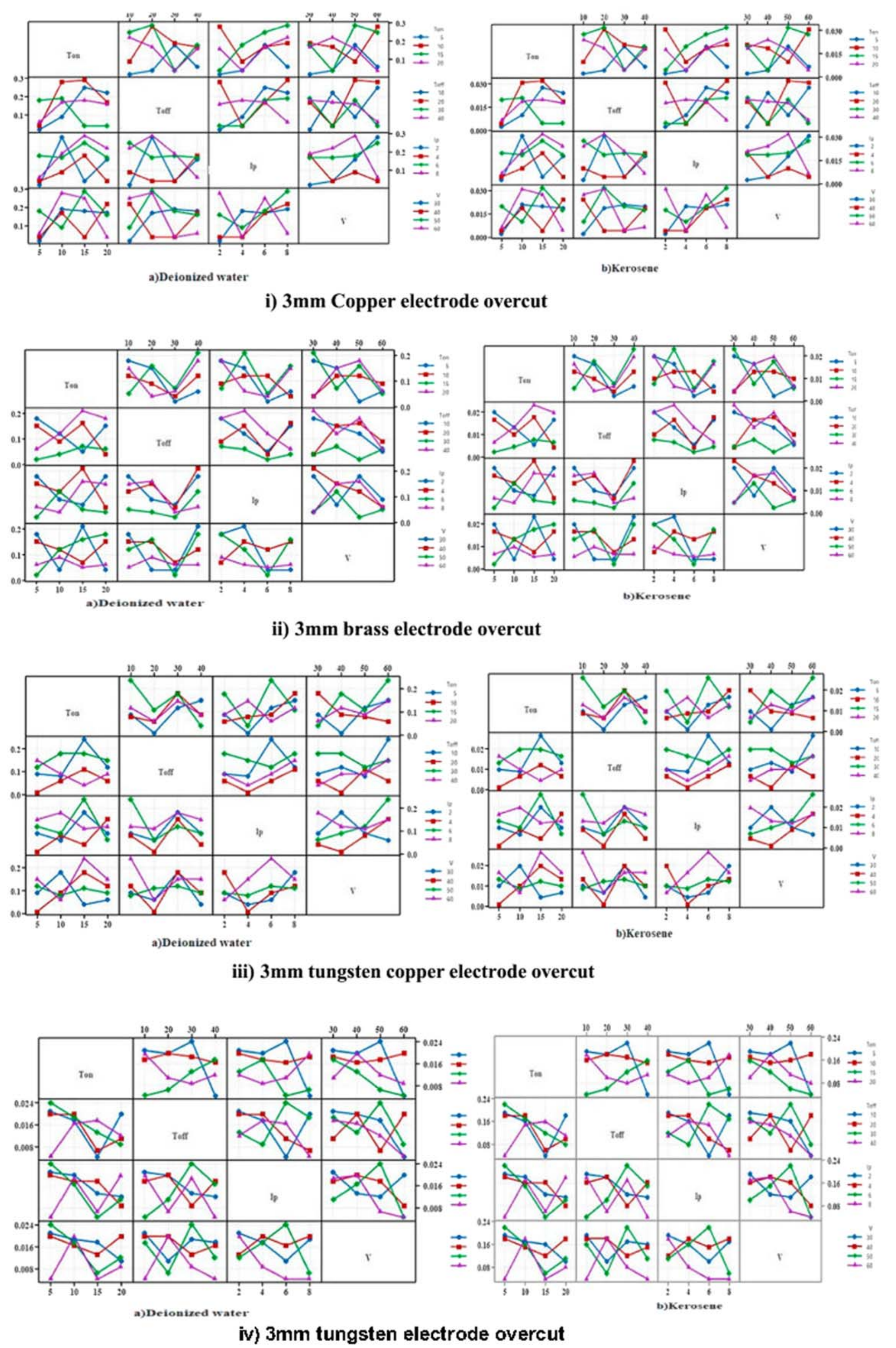

Figure 10. Overcut interaction plot for different dielectric fluid and electrode materials.

on the other hand, is caused by local vaporization or melting during the discharge process, in which small pieces of material are forcibly removed. Both properties have a negative effect on the surface quality and shorten the service life of components manufactured by spark erosion. Figure 12(d) shows a grainy texture with a more

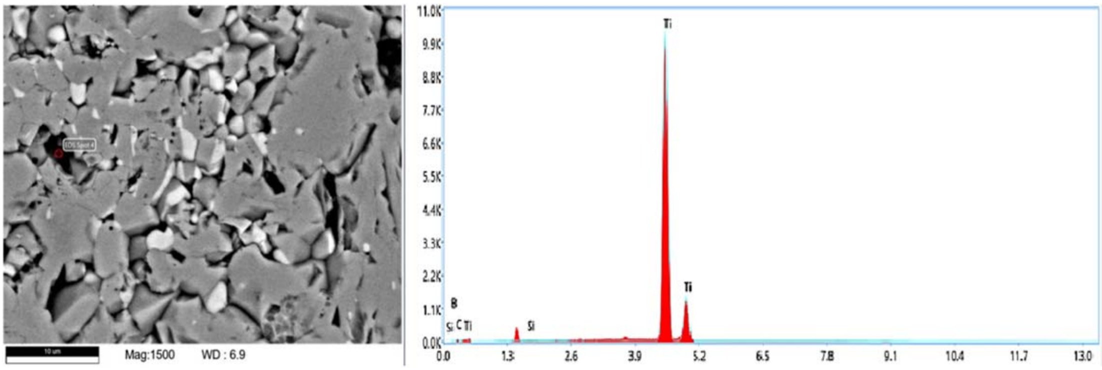

Figure 11. SEM analysis before machining and EDS analysis of titanium diboride material.

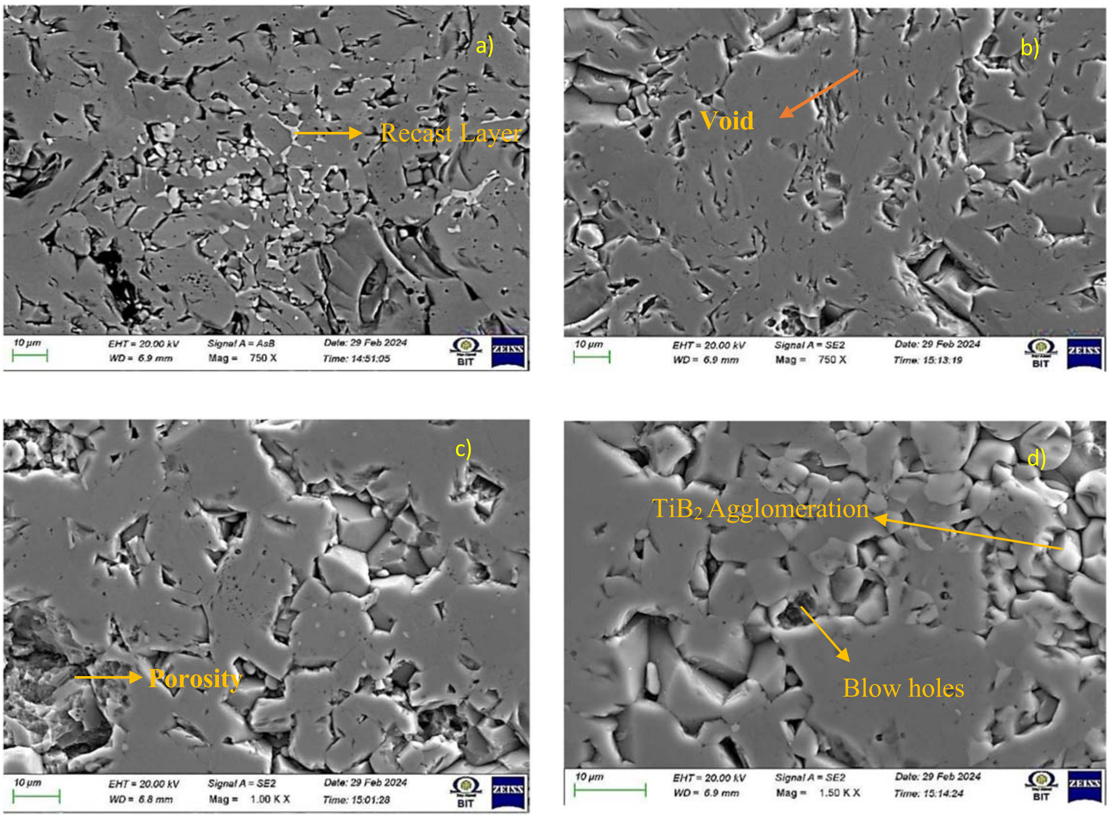

Figure 12. SEM analysis after EDM machining.

uniform distribution. This graininess could indicate redeposition of material from the tool electrodes. The EDM process not only removes workpiece material, but also results in electrode wear, which can result in tool material being deposited on the machined surface. These small, grainy deposits may be tool fragments that have stuck to the workpiece due to the intense heat [25].

6. Conclusion

In the present research work, TiB_2 material was processed using the EDM process with different processing conditions. A substantial experimental investigation is carried out to determine the EDM machinability of brass, Cu, WCu and W by modifying the input response variables T_{on}, T_{off}, I_p and V using deionized water and a kerosene dielectric medium. Both the experimental model and the regression model show that the workpiece machined with tungsten copper electrode and deionized water-based dielectric fluids has better MRR, lower overcut value, improved surface finish, and moderate TWR value. The study also shows that the holes drilled

Table 17. Result comparison with existing research work.

S. no.	Parameter	Existing research (Torres *et al*) [1, 7]	Current research
1	Electrode	Copper	Copper, brass, Tungsten copper and Tungsten
2	Dielectric fluid	Deionized water	Deionized water and kerosene
3	Material	TiB_2	TiB_2
4	Optimization technique	Anova	Regression model
5	Experiment Level	3	4
6	Voltage (V)	—	30, 40, 50, 60
7	T_{on} (μs)	5, 25, 45	5, 10, 15, 20
8	T_{off} (μs)	—	10, 20, 30, 40
9	Discharge Current	2, 4, 6	2, 4, 6, 8
10	Duty cycle	0.4, 0.5, 0.6	—
11	MRR(mm^3/min)	3.0400	3.129(tungsten copper electrode,deionized
12	TWR(mm^3/min)	1.10	0.094(Tungsten electrode, deionized water)
13	Surface Roughness (μm)	1.11	1.898(tungsten copper electrode, deionized water)
14	Overcut (mm)	—	0.008(tungsten copper electrode, kerosene)

with EDM in TiB_2 parts of gas turbine engines, landing gear and aircraft ducts [26] are machined with a tungsten copper electrode and deionized water as a dielectric fluid with high accuracy and good surface finish .The main findings of this investigation are given below

(1) The copper electrode provides better MRR and surface finish, but the tool wear rate is higher.

(2) Tungsten copper electrodes with deionized water produce better MRR, lower overcut, and moderate tool wear rate compared to the other three electrode materials .

(3) Brass electrodes produce lower MRR, high TWR, high overcut value and surface roughness is also poor for both deionized water and kerosene medium.

(4) The deionized water-based dielectric medium provides better surface finish and lower TWR compared to kerosene-based medium due to better cooling rate and more effective debris flushing. whereas kerosene-based dielectric media produces better MRR due to good spark efficiency

(5) Increasing the T_{on} results in more MRR but more thermal damage and surface roughness. A high T_{off} value results in better cooling, debris removal and a lower TWR, but reduces the MRR value. Increasing V results in more MRR but also increases TWR, the surface roughness. Increasing the I_p results in a higher MRR but drastically increases the TWR and surface roughness value. Therefore, optimal I_p, T_{on}, T_{off} and V values are crucial for maintaining efficiency and surface quality when machining TiB_2 material.

(6) SEM analysis shows that Cu and WCu produce a smoother surface with fewer cracks when deionized water is used as the dielectric medium. Kerosene as a dielectric medium leaves more carbon residue on the machined surface when used with brass and copper electrodes.

Table 17 shows the comparison of the results with existing studies. To date, only Torres *et al* [1, 7] conducted EDM research on titanium diboride material using copper as an electrode and deionized water as a dielectric fluid. When we compare the results with existing research, our results show a 9% higher MRR and an 11.70% lower TWR.

This research provides important information on the machining behavior of a hard and brittle ceramic material called titanium diboride (TiB_2). It was carried out using a variety of electrode materials including copper, brass, tungsten and tungsten-copper, as well as two dielectric fluids, deionized water and kerosene. Electrical discharge machining (EDM) of high-performance ceramics presents particular challenges when it comes to achieving efficiency and precision. Due to their remarkable mechanical and thermal properties, these materials are indispensable for applications in tool making, aerospace and automotive industries. This study lays a foundation for improving EDM settings by methodically investigating the influence of electrode material and dielectric medium on machining performance indicators such as material removal rate (MRR), tool wear rate (TWR), and surface roughness (SR). The results pave the way for further studies to improve the sustainability, efficiency and accuracy of processes for producing high-performance ceramic components, as well as to identify greener dielectric alternatives, develop new electrode compositions and fine-tune machining techniques.

Funding

The manuscript was prepared without the assistance of any grands, funds or other sources as declared by the authors.

Data availability

All data generated or analyzed during this study is included in this published article.

Declarations

The authors declare that there are no conflicts of interest associated with this publication. All authors have contributed significantly to the research, analysis, and manuscript preparation. The work described is original and has not been submitted elsewhere for publication.

Ethical approval

The authors confirm that this work does not contain any studies with human participants performed by any of the authors.

Consent to participate

Not applicable.

Acknowledgment

We are grateful to the department of Aeronautical Engineering and Mechanical Engineering at Excel Engineering College for the provision of all necessary facilities.

Data availability statement

All data that support the findings of this study are included within the article (and any supplementary files).

ORCID iDs

Karthik S https://orcid.org/0000-0002-1539-5450

References

[1] Torres A, Luis C J and Puertas I 2017 EDM machinability and surface roughness analysis of TiB_2 using copper electrodes *J. Alloys Compd.* **690** 337–47
[2] Hasçalık A and Çaydaş U 2007 Electrical discharge machining of titanium alloy (Ti–6Al–4V *Appl. Surf. Sci.* **253** 9007–16
[3] Ming W, Xie Z, Cao C, Liu M, Zhang F, Yang Y, Zhang S, Sun P and Guo X 2022 Research on EDM performance of renewable dielectrics under different electrodes for machining SKD11 *Crystals* **12** 291
[4] Janardhana K, Anushkannan N K, Dinakaran K P, Puse R K and Boopathi S 2023 Experimental investigation on microhardness, surface roughness, and white layer thickness of dry EDM *Eng. Res. Express* **5** 025022
[5] Bhaumik M and Maity K 2018b Effect of electrode materials on different EDM aspects of titanium alloy *Silicon* **11** 187–96
[6] Wang X, Liu Z, Xue R, Tian Z and Huang Y 2014 Research on the influence of dielectric characteristics on the EDM of titanium alloy *The International Journal of Advanced Manufacturing Technology/International Journal, Advanced Manufacturing Technology* **72** 979–87
[7] Torres A, Luis C and Puertas I 2017 Spacing roughness parameters analysis on the EDM of TiB_2 *Procedia Manufacturing* **13** 579–84
[8] Farooq M U, Anwar S and Hurairah A 2023 Reducing micro-machining errors during electric discharge machining of titanium alloy using nonionic liquids *Mater. Manuf. Processes* **39** 449–64
[9] Arun I, Velkavrh I, Rani R U, Annamalai S and C Y 2024 Electrical discharge shape memory alloying of Ti-6Al-4V: Mechanisms and mechanical properties *Proc. Inst. Mech. Eng.* E 355–80
[10] Ramasubbu N and Ramabalan S 2023 Experimental feasibility study of coconut oil for sustainable electrical discharge machining on hastelloy B2 *Sadhana/SaDhana* **48** 137
[11] Baroi B K, Jagadish N and Patowari P K 2022 Parametric study of electric discharge machining of titanium grade 2 alloy in distilled water *Materials Today: Proceedings,* **59** 1584–90
[12] Perumal A, Azhagurajan A, Baskaran S, Prithivirajan R and Narayansamy P 2019 Statistical evaluation and performance analysis of electrical discharge machining (EDM) characteristics of hard Ti-6Al-2Sn-4Zr-2Mo alloy *Mater. Res. Express* **6** 056552

[13] Shabarinathan k T, Kumar K S, N K and Rm U 2024 Investigation of enhancing EDM machining performance of inconel alloy using composite electrodes. *Mater. Res. Express* **11** 01651

[14] Sivakumar K, Sai Prasanna Kumar J, Loganathan K, Mugendiran V, Maridurai T and Suresh K 2022 Machining characteristics of silane-treated wheat husk biosilica in deionized water dielectric on EDM drilling of Ti-6Al-4 V alloy *Biomass Conversion and Biorefinery* **14** 199–206

[15] Rakshaskar R and Kannan C 2024 Enhancing surface integrity and performance of EDM with sustainable dielectrics and electrode modifications *Eng. Res. Express* **6** 025526

[16] Satija D, Bhute P, Gohil V and Meshram D B 2023b A study in electrical discharge machining using copper tungsten electrode *Mater. Today Proc.* (https://doi.org/10.1016/j.matpr.2023.01.043)

[17] Sawant S N, Patil S K, Unune D R, Nazare P and Wojciechowski S 2023 Effect of copper, tungsten copper and tungsten carbide tools on micro-electric discharge drilling of Ti–6Al–4V alloy *Journal of Materials Research and Technology* **24** 4242–57

[18] Darji Y, Patel D, Patel D, Ramesh R, Oza A D, Bhole K S, Shinde S M , and Kumar , M 2023 Experimentation with the EDM parameter through a full factorial technique and optimization using regression analysis with carbon nanotubes *IJIDEM* 1–14

[19] Hema P, Naveena K and Chaitanya Y 2022 Parametric optimization of process parameters on performance characteristics using die-sinking EDM with deionized water and kerosene as dielectrics. *Materials Today: Proceedings* **62** 655–64

[20] Kt S, Kumar K S, N K and Rm U 2024b Investigation of enhancing EDM machining Performance of inconel alloy using composite electrodes *Mater. Res. Express* **11** 016513

[21] Hegde A L, Shetty R, Nayak R and Shetty S 2024 Design of experiments integrated with neural networks for optimization and predictive modelling of electrode wear of novel Ti- 6Al-4V-SiCp composites during die sinking electric discharge machining *Mater. Res. Express* **11** 056522

[22] Karthik S, Karunakaran P and Velmurugan G 2024 Experimental Investigation of WE43(T6) magnesium metal matrix composites to enhance mechanical properties and EDM process parameters *Int. J. Electrochem. Sci.* **19** 100553

[23] Kumar R, Yadav V, Rawal L and Kulshrestha U 2022 Analysis of over cut in electrical discharge machining of nickel-based alloy using Taguchi approach *Mater. Manuf. Processes* **38** 126–34

[24] Sivakumar A, Saravanan K, Navaneethakrishnan P and Sekar R R 2012 Globalisation effect of productivity and quality dimensions on capacity utilisation through multivariate confirmatory analysis *International Journal of Enterprise Network Management* **5** 355

[25] Moghanizadeh A 2016 Reducing side overcut in EDM process by changing electrical field between tool and work piece *The International Journal of Advanced Manufacturing Technology* **90** 1035–42

[26] Inagaki I, Takechi T, Shirai Y and Ariyasu N 2014b *Application and features of titanium for the aerospace industry, Nippon Steel and Sumitomo Metal Technical Report 106* 22–7 (https://nipponsteel.com/en/tech/report/nssmc/pdf/106-05.pdf)